

# The Dependence of Galaxy Luminosity Function on Large-Scale Environment

H.J. Mo<sup>1</sup>, Xiaohu Yang<sup>1,2</sup>, Frank C. van den Bosch<sup>3,4</sup>, Y.P. Jing<sup>5</sup> <sup>★</sup>

<sup>1</sup> *Department of Astronomy, University of Massachusetts, Amherst MA 01003-9305, USA*

<sup>2</sup> *Center for Astrophysics, University of Science and Technology of China, Hefei, Anhui 230026, China*

<sup>3</sup> *Institute of Astronomy, Swiss Federal Institute of Technology, ETH Hönggerberg, CH-8093, Zurich, Switzerland*

<sup>4</sup> *Max-Planck-Institut für Astrophysik Karl-Schwarzschild-Strasse 1, 85748 Garching, Germany*

<sup>5</sup> *Shanghai Astronomical Observatory; the Partner Group of MPA, Nandan Road 80, Shanghai 200030, China*

## ABSTRACT

A basic assumption in current halo occupation model is that the properties of a galaxy depend only on the mass of its dark matter halo. An important consequence of this is that the segregation of the galaxy population by large-scale environment is entirely due to the environmental dependence of the halo population. In this paper we use such a model to predict how the galaxy luminosity function depends on large-scale environment. The latter is represented by the density contrast ( $\delta$ ) averaged over a spherical volume of radius  $R = 8 h^{-1} \text{Mpc}$ . The model predicts that the Schechter function is a good approximation to the luminosity functions of galaxies brighter than  $\sim 10^9 h^{-2} L_{\odot}$  ( $b_j$ -band) in virtually all environments. The characteristic luminosity,  $L^*$ , increases moderately with  $\delta$ . The faint-end slope,  $\alpha$ , on the other hand, is quite independent of  $\delta$ . However, when splitting the galaxy population into early and late types, it is found that for late-types  $\alpha$  is virtually constant, whereas for early-types  $\alpha$  increases from  $\sim 0$  in underdense regions ( $\delta \sim -0.5$ ) to  $\sim -1$  in highly overdense regions with  $\delta \sim 10$ . The luminosity function at  $L_{b_j} < 10^9 h^{-2} L_{\odot}$  is significantly steeper than the extrapolation of the Schechter function that fits the brighter galaxies. This steepening is more significant for early-types and in low-density environments. The model also predicts that the luminosity density and mass density are closely correlated. The relation between the two is monotonic but highly non-linear. This suggests that one can use the luminosity density, averaged over a large volume, to rank the mass density. This, in turn, allows the environmental effects predicted here to be tested by observations.

**Key words:** dark matter - large-scale structure of the universe - galaxies: haloes - methods: statistical

## 1 INTRODUCTION

In a hierarchical cosmogony like the cold dark matter (CDM) model, galaxies are assumed to form in dark matter haloes (e.g. White & Rees 1978). A generic prediction of such cosmogony is that the properties of the galaxy population must be closely related to that of the halo population. If the cosmological density field is Gaussian and if the power of density perturbations extends to large scales, as is the case in the current CDM cosmogony, halo properties are expected to be correlated to some degree with the large-scale structure, and so the properties of the galaxy population are also expected to change with large-scale environment. With high-resolution numerical simulations much has been

learned about the halo population. It turns out that a strong correlation with the large-scale environment exists only for halo mass; all other important halo properties are at most weakly correlated with the large-scale environment at any given time (e.g. Lemson & Kauffmann, 1999). This result, combined with our current model of galaxy formation, implies that the environmental dependence of the galaxy population is mainly due to the change of the halo mass function with large-scale environment. We can therefore hope to understand the environmental dependence of the galaxy population by understanding how galaxies occupy dark haloes of different masses. This is indeed the approach taken by the so-called halo occupation models, in which the *number* of galaxies per halo is assumed to depend on halo *mass* only (e.g. Jing, Mo & Börner 1998; Peacock & Smith 2000; Seljak 2000; Scoccimarro et al. 2001; Bullock, Wechsler & Som-

<sup>★</sup> E-mail: hjmo@nova.astro.umass.edu

merville 2002; Berlind & Weinberg 2002; Kang et al. 2002; Zheng et al. 2002; Yang, Mo & van den Bosch 2003a; van den Bosch, Yang & Mo 2003; Magliocchetti & Porciani 2003; Scranton 2002; Zehavi et al. 2003; Yan, Madgwick & White 2003; Kravtsov et al. 2003). Note that this assumption is non-trivial, as it implies that galaxy formation is largely a local process in individual dark matter haloes.

To test the validity of this assumption, we use the halo occupation model recently developed by Yang et al. (2003a), which is based on the conditional luminosity function (hereafter CLF) of galaxies in dark haloes of given mass, to predict how the galaxy luminosity function (hereafter LF) changes with large-scale environment. In this model, the change of the LF with large-scale environment is entirely due to the change of the halo mass function with large-scale environment. Since the conditional mass function of dark matter haloes can be accurately obtained from cosmological  $N$ -body simulation, the CLF model can be used to make accurate predictions for how the galaxy LF changes with large-scale density field. We also show that, when averaged over a large volume, the predicted galaxy luminosity density is closely correlated with the underlying mass density. Therefore, the luminosity density can be used to rank the mass density, and the model predictions presented here can be tested using large galaxy redshift surveys, such as the two-degree Field Galaxy Redshift Survey (2dFGRS; Colless et al. 2001) and the Sloan Digital Sky Survey (SDSS; York et al. 2000).

The paper is arranged as follows. In Section 2 we review the CLF model and describe how it can be used to calculate the LF of galaxies in different environments. Section 3 presents the model predictions for how the galaxy LF changes with large-scale density field. In Section 4 we use our model to study the correlation between the galaxy luminosity density and the underlying mass density, and discuss how the predictions of our CLF formalism can be tested with observations. We summarize our results in Section 5.

## 2 FROM THE CONDITIONAL LUMINOSITY FUNCTION TO GALAXY LUMINOSITY FUNCTION

In Yang, Mo & van den Bosch (2003a, hereafter Paper I), we developed a formalism, based on the conditional luminosity function  $\Phi(L|M)$ , to link the distribution of galaxies to that of dark matter haloes. We introduced a parameterized form for  $\Phi(L|M)$  which we constrained using the LF and the correlation lengths as function of luminosity. In van den Bosch, Yang & Mo (2003a, hereafter Paper II), we extended our model by constructing separate CLFs for the early- and late-type galaxies. The CLF formalism developed in these two papers has subsequently been used to investigate galaxy clustering as function of luminosity and type (Yang et al. 2003b), to put constraints on cosmological parameters (van den Bosch, Mo & Yang 2003b), to constrain redshift-evolution in the halo model (Yan, Madgwick & White 2003), and to characterize the population of satellite galaxies (van den Bosch et al. 2004). In this paper, we use the CLF formalism to predict how the luminosity function of galaxies depends on large-scale environment. For completeness, we briefly summarize in the following the main

ingredients of the CLF formalism, and we refer the reader to papers I and II for more details.

The conditional luminosity function  $\Phi(L|M)dL$  gives the average number of galaxies with luminosities in the range  $L \pm dL/2$  that reside in haloes of mass  $M$ . It is parameterized by a Schechter function:

$$\Phi(L|M)dL = \frac{\tilde{\Phi}^*}{\tilde{L}^*} \left( \frac{L}{\tilde{L}^*} \right)^{\tilde{\alpha}} \exp(-L/\tilde{L}^*) dL, \quad (1)$$

where  $\tilde{L}^* = \tilde{L}^*(M)$ ,  $\tilde{\alpha} = \tilde{\alpha}(M)$  and  $\tilde{\Phi}^* = \tilde{\Phi}^*(M)$  are all functions of halo mass  $M$ . Following Papers I and II, we write the average total mass-to-light ratio of a halo with mass  $M$  as

$$\left\langle \frac{M}{L} \right\rangle (M) = \frac{1}{2} \left( \frac{M}{L} \right)_0 \left[ \left( \frac{M}{M_1} \right)^{-\gamma_1} + \left( \frac{M}{M_1} \right)^{\gamma_2} \right], \quad (2)$$

which has four free parameters: a characteristic mass  $M_1$ , for which the mass-to-light ratio is equal to  $(M/L)_0$ , and two slopes,  $\gamma_1$  and  $\gamma_2$ , that specify the behavior of  $\langle M/L \rangle$  at the low and high mass ends, respectively. A similar parameterization is adopted for the characteristic luminosity  $\tilde{L}^*(M)$ :

$$\frac{M}{\tilde{L}^*(M)} = \frac{1}{2} \left( \frac{M}{L} \right)_0 f(\tilde{\alpha}) \left[ \left( \frac{M}{M_1} \right)^{-\gamma_1} + \left( \frac{M}{M_2} \right)^{\gamma_3} \right], \quad (3)$$

with

$$f(\tilde{\alpha}) = \frac{\Gamma(\tilde{\alpha} + 2)}{\Gamma(\tilde{\alpha} + 1, 1)}. \quad (4)$$

Here  $\Gamma(x)$  is the Gamma function and  $\Gamma(a, x)$  the incomplete Gamma function. This parameterization has two additional free parameters: a characteristic mass  $M_2$  and a power-law slope  $\gamma_3$ . For  $\tilde{\alpha}(M)$  we adopt a simple linear function of  $\log(M)$ ,

$$\tilde{\alpha}(M) = \alpha_{15} + \eta \log(M_{15}), \quad (5)$$

with  $M_{15}$  the halo mass in units of  $10^{15} h^{-1} M_\odot$ ,  $\alpha_{15} = \tilde{\alpha}(M_{15} = 1)$ , and  $\eta$  describes the change of the faint-end slope  $\tilde{\alpha}$  with halo mass. Note that once  $\tilde{\alpha}(M)$  and  $\tilde{L}^*(M)$  are given, the normalization of the conditional LF,  $\tilde{\Phi}^*(M)$ , is obtained through equations (1) and (2), using the fact that the total (average) luminosity in a halo of mass  $M$  is

$$\langle L \rangle (M) = \int_0^\infty \Phi(L|M) L dL = \tilde{\Phi}^* \tilde{L}^* \Gamma(\tilde{\alpha} + 2). \quad (6)$$

Finally, we introduce the mass scale  $M_{\min}$  below which we set the CLF to zero; i.e., we assume that no stars form inside haloes with  $M < M_{\min}$ . Motivated by reionization considerations (see Paper I for details) we adopt  $M_{\min} = 10^9 h^{-1} M_\odot$  throughout.

In order to split the galaxy population in early and late types, we follow Paper II and introduce the function  $f_{\text{late}}(L, M)$ , which specifies the fraction of galaxies with luminosity  $L$  in haloes of mass  $M$  that are late-type. The CLFs of late- and early-type galaxies are then given by

$$\Phi_{\text{late}}(L|M)dL = f_{\text{late}}(L, M) \Phi(L|M)dL \quad (7)$$

and

$$\Phi_{\text{early}}(L|M) dL = [1 - f_{\text{late}}(L, M)] \Phi(L|M) dL. \quad (8)$$

As with the CLF for the entire population of galaxies,  $\Phi_{\text{late}}(L|M)$  and  $\Phi_{\text{early}}(L|M)$  are constrained by 2dFGRS

measurements of the LFs and the correlation lengths as function of luminosity. We assume that  $f_{\text{late}}(L, M)$  has a quasi-separable form

$$f_{\text{late}}(L, M) = g(L) h(M) q(L, M). \quad (9)$$

Here

$$q(L, M) = \begin{cases} 1 & \text{if } g(L) h(M) \leq 1 \\ \frac{1}{g(L) h(M)} & \text{if } g(L) h(M) > 1 \end{cases} \quad (10)$$

is to ensure that  $f_{\text{late}}(L, M) \leq 1$ . We adopt

$$g(L) = \frac{\hat{\Phi}_{\text{late}}(L)}{\hat{\Phi}(L)} \frac{\int_0^\infty \Phi(L|M) n(M) dM}{\int_0^\infty \Phi(L|M) h(M) n(M) dM} \quad (11)$$

where  $n(M)$  is the halo mass function (Sheth & Tormen 1999; Sheth, Mo & Tormen 2001),  $\hat{\Phi}_{\text{late}}(L)$  and  $\hat{\Phi}(L)$  correspond to the *observed* LFs of the late-type and entire galaxy samples, respectively, and

$$h(M) = \max \left( 0, \min \left[ 1, \left( \frac{\log(M/M_a)}{\log(M_b/M_a)} \right) \right] \right) \quad (12)$$

with  $M_a$  and  $M_b$  two additional free parameters, defined as the masses at which  $h(M)$  takes on the values 0 and 1, respectively. As shown in Paper II, this parameterization allows the population of galaxies to be split in early- and late-types such that their respective LFs and clustering properties are well fitted.

In Papers I and II we presented a number of different CLFs for different cosmologies and different assumptions regarding the free parameters. In what follows we focus on the flat  $\Lambda$ CDM cosmology with  $\Omega_m = 0.3$ ,  $\Omega_\Lambda = 0.7$  and  $h = H_0/(100 \text{ km s}^{-1} \text{ Mpc}^{-1}) = 0.7$  and with initial density fluctuations described by a scale-invariant power spectrum with normalization  $\sigma_8 = 0.9$ . These cosmological parameters are in good agreement with a wide range of observations, including the recent WMAP results (Spergel et al. 2003), and in what follows we refer to it as the ‘‘concordance’’ cosmology. Finally, we adopt the CLF with the following parameters:  $M_1 = 10^{10.88} h^{-1} M_\odot$ ,  $M_2 = 10^{12.27} h^{-1} M_\odot$ ,  $M_a = 10^{17.30} h^{-1} M_\odot$ ,  $M_b = 10^{7.87} h^{-1} M_\odot$ ,  $(M/L)_0 = 172h \text{ (M/L)}_\odot$ ,  $\gamma_1 = 2.38$ ,  $\gamma_2 = 0.25$ ,  $\gamma_3 = 0.72$ ,  $\eta = -0.22$  and  $\alpha_{15} = -1.16$ . As shown in paper II, this model (referred to as model D) yields excellent fits to the observed LFs and the observed correlation lengths as function of both luminosity and type. We emphasize, however, that our results are not sensitive to uncertainties in the CLF; had we chosen models A, B or C in paper II, instead of model D, the results presented below would have been virtually identical. Since  $\Phi(L|M)$  is the average number of galaxies per unit luminosity in a halo with mass  $M$ , one can obtain the galaxy LF,  $\Phi(L)$ , from the halo mass function,  $n(M)$ , according to

$$\Phi(L) = \int \Phi(L|M) n(M) dM. \quad (13)$$

Fig.1 shows how haloes of different masses contribute to the total luminosity function. Note that the shape of the CLF changes significantly with halo mass, and that the faint end of the LF is dominated by galaxies hosted by low-mass haloes.

If we make the assumption that the CLF is statistically independent of the large scale environment, the galaxy LF in a region of overdensity  $\delta$  follows from

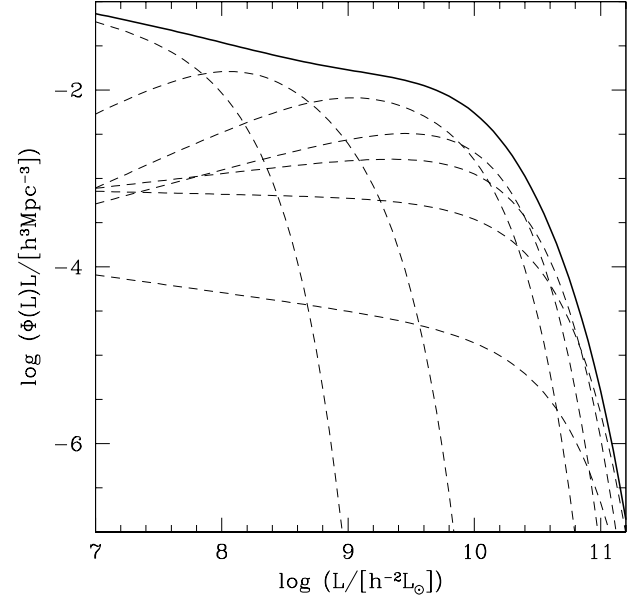


**Figure 1.** The contribution to the total luminosity function (solid curve) by haloes in various mass ranges:  $M/[h^{-1} M_\odot] \leq 5 \times 10^{10}$ ,  $5 \times 10^{10} - 10^{11}$ ,  $10^{11} - 10^{12}$ ,  $10^{12} - 10^{13}$ ,  $10^{13} - 10^{14}$ ,  $10^{14} - 10^{15}$ ,  $> 10^{15}$  (broader curve corresponds to larger mass).

$$\Phi(L|\delta) = \int \Phi(L|M) n(M|\delta) dM. \quad (14)$$

Here  $n(M|\delta)$  is the conditional mass function of dark matter haloes, which gives the number density of haloes as a function of halo mass in an environment with average mass overdensity  $\delta \equiv [\mathcal{M} - \overline{\mathcal{M}}]/\overline{\mathcal{M}}$  (with  $\mathcal{M}$  the total mass in volume  $V$ , and  $\overline{\mathcal{M}}$  the mean mass in all volumes  $V$ ). Thus, in the CLF formalism, the  $\delta$ -dependence of the galaxy LF enters only through the conditional mass function  $n(M|\delta)$ .

Fig.2 shows the conditional mass functions for haloes in several representative environments. These functions are derived from a high-resolution  $N$ -body simulation which follows the motions of  $512^3$  particles with a  $P^3M$  code in a  $100h^{-1} \text{ Mpc}$  box (see Jing & Suto 2002 for details), assuming the  $\Lambda$ CDM ‘concordance’ cosmology specified above. Dark matter haloes are identified using the standard friends-of-friends algorithm with a linking length of 0.2 times the mean inter-particle separation. As one can see, the shape of the conditional mass function is quite independent of  $\delta$  at the low mass end, while the shape at the high-mass end depends significantly on  $\delta$ . The break in the conditional mass function at the high-mass end occurs at a lower mass for lower  $\delta$ . This reflects the fact that the formation of massive haloes is suppressed in low density regions due to bias (e.g. Mo & White 1996; Gottloeber et al. 2003). For a given  $\delta$ , the break occurs at smaller mass if the volume used to define  $\delta$  is smaller.

Ideally, if we have an accurate model for the conditional mass function, we can combine it with the conditional luminosity function to construct an analytical model for the  $\delta$ -dependence of the galaxy LF. Unfortunately, the model based on peak-background splitting (e.g. Mo & White 1996)

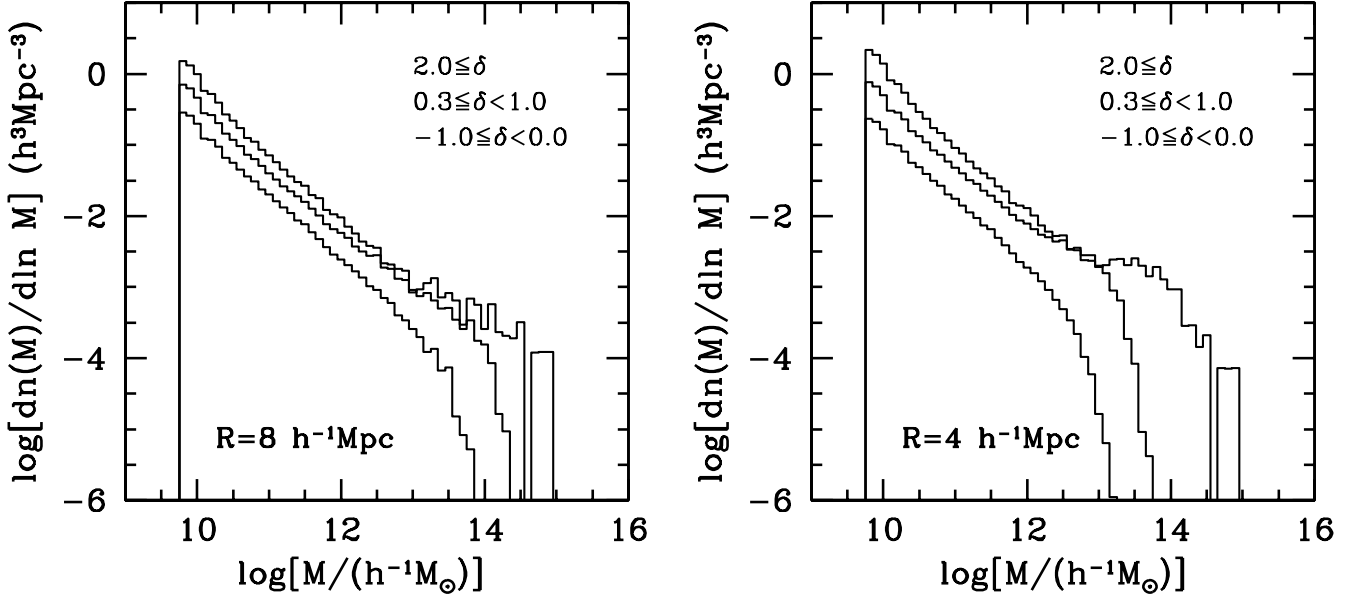


**Figure 2.** The conditional mass functions of dark matter haloes in various environments, specified by the mass overdensity  $\delta$  in a spherical volume with radius  $R = 8h^{-1}$  Mpc (left-hand panel) and  $R = 4h^{-1}$  Mpc (right-hand panel).

is not sufficiently accurate for our purpose, even if ellipsoidal collapse is taken into account (Sheth, Mo & Tormen 2001; Sheth & Tormen 2002). The reason for this is that, when the total mass contained in a volume becomes comparable to the mass of individual haloes in consideration, as is the case for massive haloes in low-density volumes, the peak-background splitting becomes inaccurate (e.g. Sheth & Tormen 2002). We therefore decided to use the simulated samples constructed in Yang et al. (2003b) for our purpose. These simulated samples were obtained by populating dark matter haloes in  $N$ -body simulations with galaxies according to the CLF model described above. Here we use the sample constructed from one of the  $100 h^{-1}$  Mpc simulations, which is complete down to a  $b_J$ -band luminosity of  $L_{b_J} \sim 10^8 h^{-2} L_\odot$  (see Yang et al. 2003b for details).

### 3 GALAXY LUMINOSITY FUNCTION IN DIFFERENT ENVIRONMENTS

Fig. 3 shows the LFs of galaxies in regions of different mass overdensities  $\delta$  (defined over spheres with radius  $R = 8h^{-1}$  Mpc). As one can see, the *shape* of the LF at the faint end is quite independent of  $\delta$ . This is due to the fact that most faint galaxies reside in low mass haloes, for which the *shape* of the conditional mass function  $n(M|\delta)$  is only weakly dependent on  $\delta$  (cf. Fig. 2). The most pronounced difference between LFs in different mass density environments is the break at the bright end, which occurs at fainter luminosities in lower-density regions. This, in turn, is simply a reflection of the fact that most bright galaxies reside in massive haloes.

Our CLF model also predicts a pronounced difference for the environment dependence of the LFs of early- and late-type galaxies. As shown in Fig. 4, the *shape* of the LF of early-type galaxies depends rather strongly on  $\delta$ . For the late-type galaxies, however, no such pronounced shape-dependence is predicted. Once again, this behaviour is easy

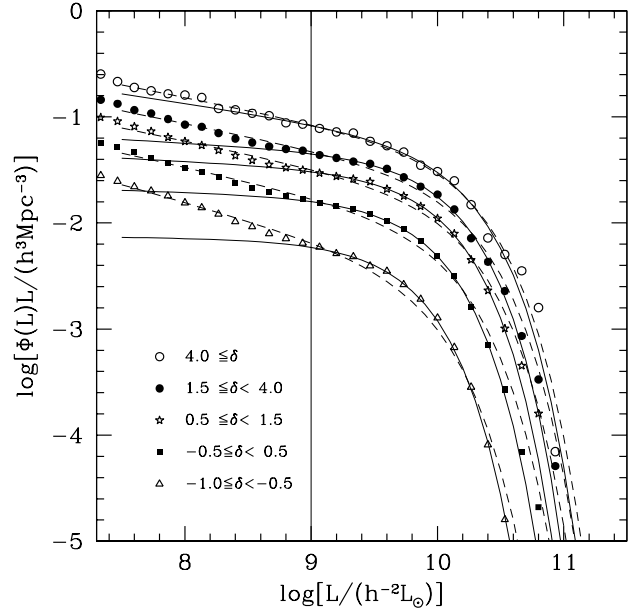


**Figure 3.** Galaxy luminosity functions in regions with different mass overdensities:  $-1.0 \leq \delta < -0.5$  (open triangles),  $-0.5 \leq \delta < 0.5$  (solid squares),  $0.5 \leq \delta < 1.5$  (asterisks),  $1.5 \leq \delta < 4.0$  (solid circles), and  $\delta \geq 4.0$  (open circles). The solid and dashed curves correspond to the best-fit Schechter functions, fit over the luminosity ranges  $L_{b_J} \geq 10^9 h^{-2} L_\odot$  and  $L_{b_J} \geq 10^{7.5} h^{-2} L_\odot$ , respectively.

to understand from the conditional halo mass function and the CLF: many of the fainter early-types actually reside in clusters (see Paper II), whose abundance depends strongly on  $\delta$ . The majority of the faint late-type galaxies, on the other hand, reside in relatively low mass haloes, for which

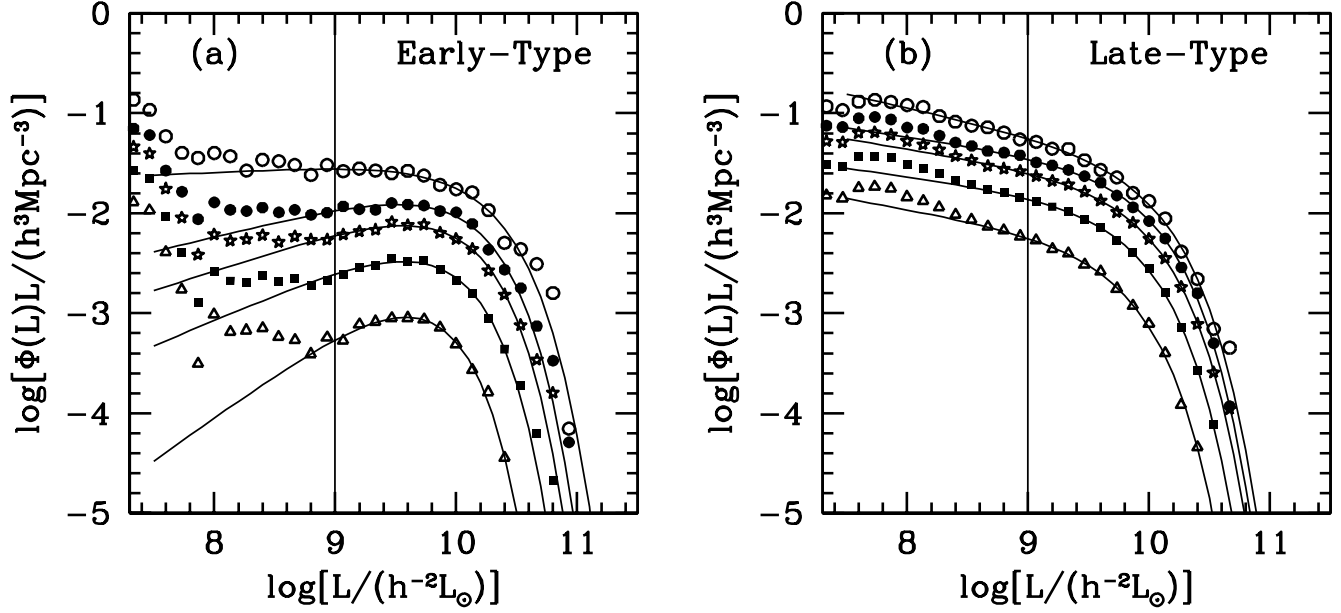


Figure 4. The same as Fig. 3, but for (a) early-type and (b) late-type galaxies. Solid curves correspond to the best-fit Schechter functions, fit over the range  $L \geq 10^9 h^{-2} L_{\odot}$ .

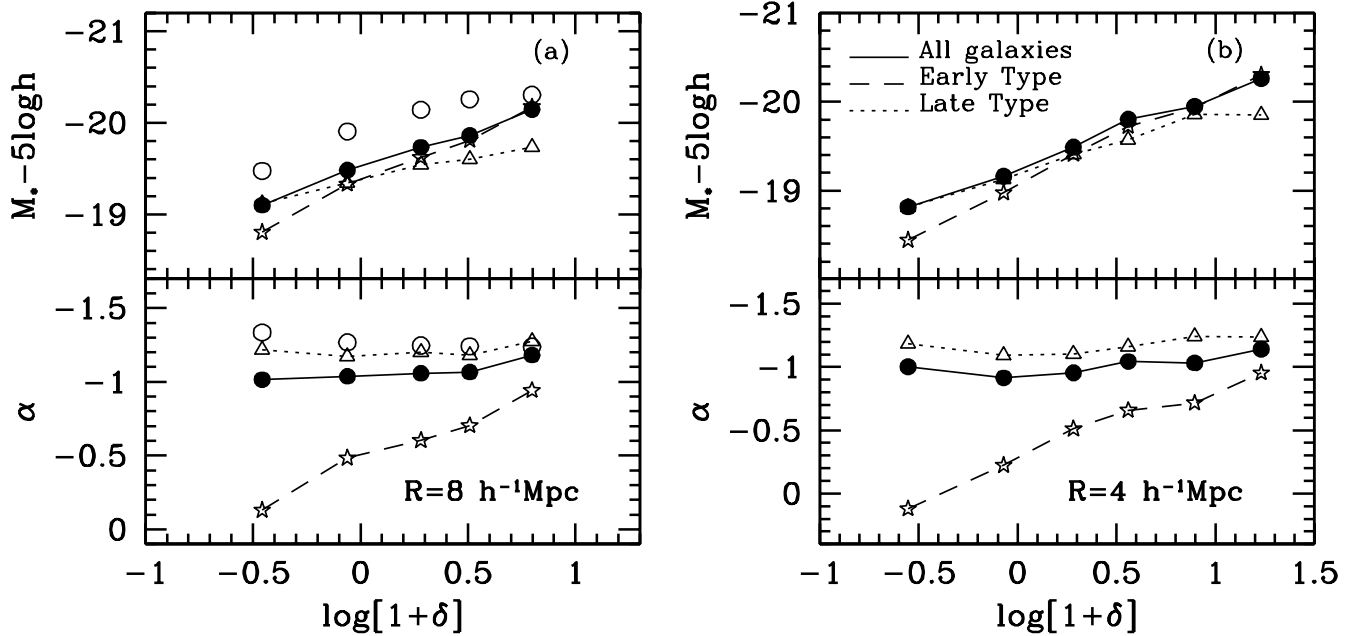
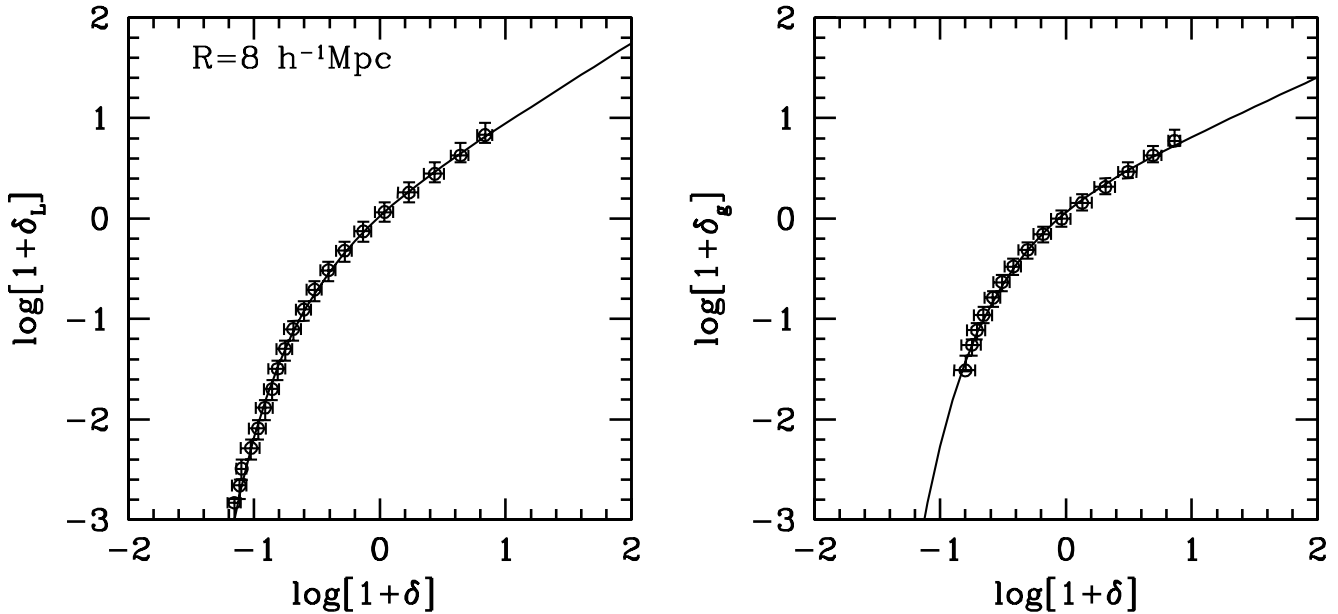


Figure 5. The characteristic luminosity and faint-end slope  $\alpha$  as a function of  $\delta$ , defined as the mean overdensity within individual spheres of radius  $R = 8 h^{-1} \text{Mpc}$  (left panel) and  $R = 4 h^{-1} \text{Mpc}$  (right panel). Symbols connected with lines are results of the fit over the luminosity range  $L \geq 10^9 h^{-2} L_{\odot}$  for the total (solid line), early-type (dashed line) and late-type (dotted line) samples. For comparison, the open circles in the left-hand panel show the results for the total sample when fitting over the more extended luminosity range  $L \geq 10^{7.5} h^{-2} L_{\odot}$ .

the shape of the conditional halo mass function is roughly independent of environment (cf. Fig.2).

To further quantify how the LF depends on the mean density of the environment, we fit each of the luminosity functions by a Schechter form. For most of our discussion, we only fit over the luminosity range  $L \geq 10^9 h^{-2} L_{\odot}$  ( $M_{b_j} - 5 \log h \lesssim -17.2$ ). In real redshift surveys, such as

the 2dFGRS, galaxies fainter than this are observed only within a relatively small local volume, making it difficult to study their large-scale environment dependencies. As shown in Figs. 3 and 4, the Schechter function provides in general a reasonable fit to the LF over a large range in luminosity. This is not a trivial result, as the shape of the CLF varies



**Figure 6.** The left panel shows the relation between luminosity density ( $\delta_L$ , calculated using all galaxies resolved in the simulation) and mass density ( $\delta$ ), while the right panel shows the galaxy number density ( $\delta_g$ , calculated using galaxies with luminosity  $L \geq 10^9 h^{-2} L_\odot$ ). All quantities are the averages within a sphere of radius  $R = 8 h^{-1} \text{Mpc}$ , and normalized to the corresponding mean densities of the universe. The curves show the fits to the relations. Error bars for  $\delta_L$  and  $\delta_g$  represent the ranges of the quantities, while errorbars for  $\delta$  are  $1\sigma$  standard deviations. Note that below a certain value of  $\delta$ ,  $\log(1 + \delta_g)$  becomes  $-\infty$ , while  $\log(1 + \delta_L)$  is still finite.

significantly with halo mass and the conditional mass function at the high-mass end changes significantly with  $\delta$ .

The left panel of Fig. 5 shows the characteristic luminosity  $L^*$  and the faint end slope  $\alpha$  as functions of  $\delta$ . In all cases, the characteristic luminosity increases with  $\delta$ , reflecting the fact that massive haloes, which host bright galaxies, are preferentially located in high-density regions. The increase is only moderate: for the total sample it is about one magnitude from the lowest to the highest densities probed. The increase is more significant for early-type galaxies than for late-type galaxies. For late-type galaxies, the increase becomes insignificant for  $\delta \gtrsim 1$ .

For the total population the faint-end slope  $\alpha$  is roughly a constant, with a value about  $-1.1$ . The faint-end slope is also quite independent of  $\delta$  for late-type galaxies, with  $\alpha \sim -1.25$ . In contrast, the faint-end slope for early-type galaxies changes from  $\alpha \sim 0$  for very low density regions to  $\alpha \sim -1$  for  $\delta \sim 10$ . As mentioned above, this is mainly due to the fact that a large number of relatively faint early types reside in massive haloes whose mass function depends strongly on  $\delta$ .

If we fit the luminosity function over the entire range with  $L \gtrsim 10^{7.5} h^{-2} L_\odot$  ( $M_{b_j} - 5 \log h \lesssim -13.5$ ), the faint-end slope becomes steeper for low-density regions (cf. open and solid circles in left-panel of Fig. 5). Note that in this case, the Schechter function is no longer a good fit (see Fig. 3) for low-density regions; the faint-end slope is much steeper than that of the extrapolation from the luminosity function at the brighter end. This departure starts at  $L \sim 10^9 h^{-2} L_\odot$  and is more significant for early-type galaxies.

We have also made similar analyses for spherical volumes with a radius of  $4 h^{-1} \text{Mpc}$ , the results of which are shown in the right-hand panel of Fig. 5. A noticeable dif-

ference with using volumes of  $8 h^{-1} \text{Mpc}$  radius is that the characteristic luminosity increases faster with  $\delta$ . The reason is that the conditional mass function at the high-mass end reveals a stronger dependence on  $\delta$  for smaller radius  $R$  (see Fig. 2).

#### 4 PREDICTIONS FOR OBSERVATIONAL TESTS

So far we have investigated how the galaxy LF depends on the mass density averaged over spherical volumes of  $8 h^{-1} \text{Mpc}$  radius. Unfortunately, it is not easy observationally to obtain accurate measures for the mass density field in the Universe. Therefore, in order to facilitate an observational test of the predictions presented above, we need to find a quantity that is (i) easy to derive from observations, and (ii) that can be used to rank the mass density.

When averaged within a large volume, the *number* density,  $\delta_g$  of galaxies (with luminosities above some value) and the luminosity density,  $\delta_L$ , are both expected to be correlated with the underlying mass density. Such relations can be derived directly from the simulated catalogs constructed with the CLF (Yang et al. 2003b). Fig. 6 shows the results. As one can see, there is a tight correlation between the luminosity overdensity  $\delta_L$  and mass overdensity  $\delta$ . Here  $\delta_L$  is calculated using all galaxies with  $L \geq L_{\min} = 10^7 h^{-2} L_\odot$ , but it is not sensitive to this lower limit as long as  $L_{\min} \lesssim 10^9 h^{-2} L_\odot$ . Thus the luminosity density can be used to rank the mass density. The use of galaxy *number* density is trickier, because the scatter is quite large for low-density volumes (for example,  $\delta_g$ , here defined by all galaxies with  $L \geq 10^9 h^{-2} L_\odot$ , becomes zero at  $\delta < -0.8$  in the right panel of Fig. 6) and because it depends on the luminosity

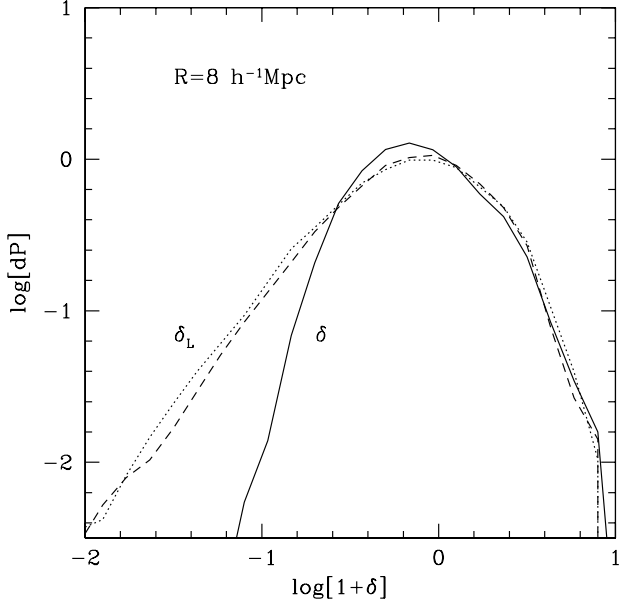


**Figure 7.** The solid and dashed curves show the distribution functions of the mass overdensity  $\delta$  and of the luminosity density  $\delta_L$ , respectively. The dotted curve shows the conversion of the distribution of mass density to the distribution of luminosity density using the mean  $\delta_L$ - $\delta$  relation shown in Fig. 6.

range used in defining the galaxy overdensity  $\delta_g$  (since the number density of galaxies is dominated by the faint ones).

In order to show that  $\delta_L$  can be used to rank  $\delta$ , we first fit the mean  $\rho_L$ - $\rho$  relation by the following function

$$y = Ae^{-x_*} x^\beta e^{x_*/x}, \quad (15)$$

where  $x = 1 + \delta$ ,  $y = 1 + \delta_L$ , and  $A$ ,  $x_*$  and  $\beta$  are fitting parameters. For high-density cells ( $x \gg x_*$ ),  $y \propto x^\beta$ , while for  $x \ll x_*$ ,  $y$  decreases exponentially with decreasing  $x$ . For  $R = 8 h^{-1} \text{Mpc}$ , we obtain  $A = 1.0545$ ,  $x_* = -0.3643$  and  $\beta = 0.7835$ . We then use this mean relation to convert the distribution function of the mass density into a distribution function for the luminosity density and compare it with the luminosity-density distribution function derived directly from the simulation. The result is shown in Fig. 7. Clearly, the luminosity-density distribution function is recovered quite accurately with the mean relation (15), suggesting that the luminosity density can be used to represent the mass density.

Fig. 8 shows how  $L^*$  and  $\alpha$  change with the luminosity density. The results are similar to those shown in Fig. 5, except that the range of  $\delta_L$  is stretched at the low-density end relative to  $\delta$ , because of the non-linear relationship between  $\delta_L$  and  $\delta$ . As comparison, we also show  $L^*$  and  $\alpha$  as functions of  $\delta_g$ , where  $\delta_g$  is based on the number of galaxies with  $L \geq 10^9 h^{-2} L_\odot$  (Fig. 9). With such a luminosity limit, the results based on  $\delta_g$  are very close to those based on  $\delta_L$ .

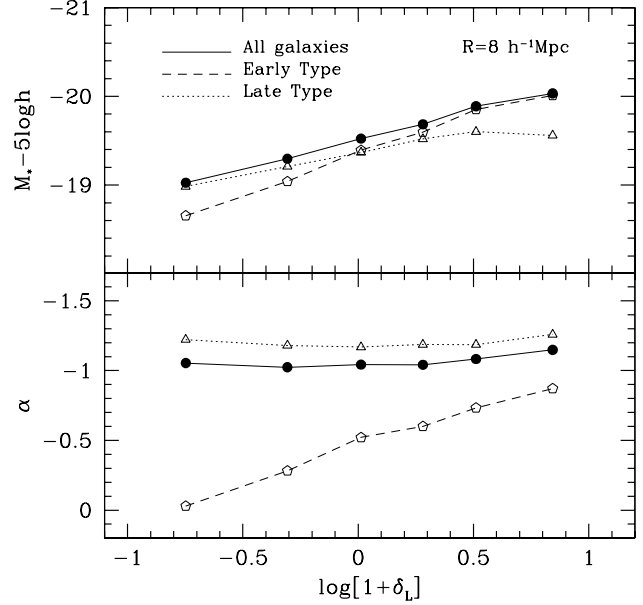


**Figure 8.** The characteristic magnitude,  $M_*$ , and the faint-end slope,  $\alpha$ , of the best-fit Schechter function as functions of  $\delta_L$ . The results are shown for the total, early-type and late-type samples, as indicated. Schechter functions are fit to the luminosity functions over the range  $L \geq 10^9 h^{-2} L_\odot$ .

## 5 DISCUSSION

We have shown that the halo occupation model, which assumes that the luminosity distribution in a dark halo only depends on its mass, makes specific predictions about how the galaxy LF changes with large-scale environment. The model predicts that the LFs for relatively bright galaxies can be fit reasonably well by a Schechter function, independent of environment. In all cases the characteristic luminosity  $L^*$  increases with local mass density. For late-type galaxies, the faint-end slope is quite independent of large-scale environment while for early-types the value of  $\alpha$  changes from  $\sim 0$  in low density regions to  $\sim 1$  in high-density regions. The predicted LF for low-density regions shows significant departure from the Schechter form at  $L \lesssim 10^9 h^{-2} L_\odot$ , and this departure is more significant for early-type galaxies. All these predictions have simple explanations based on the change of halo mass function with large-scale environment, and the change of halo occupation with halo mass.

We have also shown that the luminosity density is tightly correlated with the mass density on large scales. Thus, our predictions can be checked using large galaxy redshift surveys. At the moment, the study of the dependence of galaxy LF on local environment has mainly focused on comparing the LF of cluster galaxies with that of field galaxies (see e.g. De Propris et al. 2003 and references therein). More related to the model predictions presented here are the analyses made by Hütsi et al. (2002) and Bromley et al. (1998). Hütsi et al. estimated galaxy LFs in spherical volumes with a radius  $10 h^{-1} \text{Mpc}$  (in redshift space) within which the overdensities of galaxy number are respectively  $\delta_g < 0$ ,  $0 < \delta_g < 1$ , and  $\delta_g > 1$ , and found that the faint-

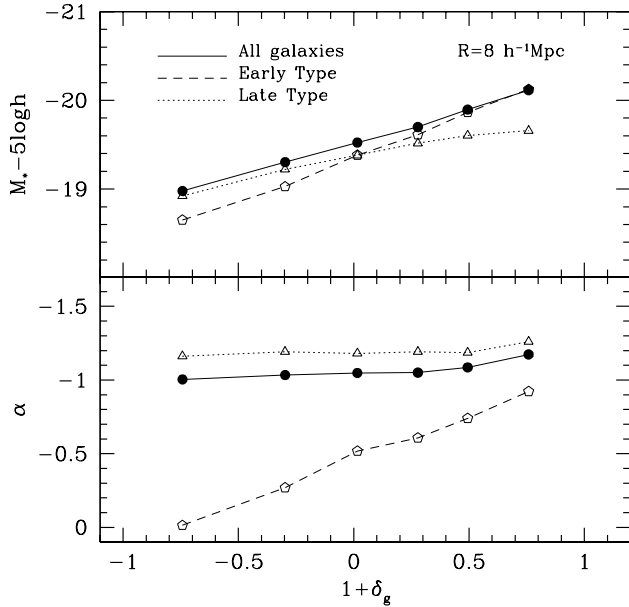


**Figure 9.** Same as Fig. 8, but as a function of  $\delta_g$ , the overdensity (in number) of galaxies with  $L \geq 10^9 h^{-2} L_\odot$ .

end slope  $\alpha$  is about  $-1.1$  for all the three cases, but that the characteristic luminosity brightens by about  $0.4$  magnitude from the lowest-density sample to the highest-density sample. These results are consistent with our model prediction. Bromley et al. found that the faint-end slope of the LF of early-type galaxies (defined according to spectral type) depends strongly on local density, with  $\alpha$  increasing from  $\sim -0.4$  in high density regions to  $\sim 0.2$  in low density regions. This trend is also consistent with our model prediction. Unfortunately, current observational results are not yet sufficiently accurate to give a stringent constraint on the model. The situation will soon change. With the use of large redshift surveys of galaxies, such as the 2dFGRS and SDSS<sup>†</sup>, one can estimate to high accuracy the galaxy luminosity functions in regions of different luminosity densities or galaxy number densities (Croton et al. in preparation), facilitating an accurate comparison between model and observations.

As far as an accurate comparison with observation is concerned, there are several effects to be taken into account. The first is redshift distortion. Since bright galaxies in massive clusters are expected to have large velocity dispersion, some of these galaxies may appear in ‘low-density’ regions in redshift space, weakening the dependence on  $\delta$ . This effect was seen in our experiment where  $\delta$  was defined in redshift space. The second is concerned with the definition of overdensity. In a magnitude-limited sample, volumes at large distances from us contain only bright galaxies, and so the es-

timate of the overdensity in such a cell has to rely on a small number of bright galaxies. Since the shape of the luminosity function changes with  $\delta$ , the correction of the incompleteness due to the magnitude limit in individual volumes must take this effect into account. Finally, since the Schechter function is not a perfect model, the fitting parameters depend on the luminosity *range* used for the fit. All these effects can be taken into account properly with the use of mock catalogs by applying the same analyses to both the simulated and observed samples. We plan to present such a detailed comparison with observational data in a forthcoming paper.

It is also interesting to compare the predictions presented here, based on the CLF, with those based on semi-analytical models for galaxy formation (e.g. Kauffmann et al. 1999; Somerville & Primack 1999; Benson et al. 2002; Mathis et al. 2002). Mathis & White (2002) have shown that the characteristic luminosity of the galaxy luminosity function in their semi-analytical model increases progressively from low-density to high-density environments while the faint-end slope becomes slightly shallower. These results are in qualitative agreement with our predictions presented here. As already emphasized in paper II, this suggests that the halo occupation statistics as described by our CLF nicely fit within the standard framework of galaxy formation.

## ACKNOWLEDGEMENT

We are grateful to Darren Croton, Glennys Farrar, and Guinevere Kauffmann for useful discussions. Numerical simulations used in this paper were carried out at the Astronomical Data Analysis Center (ADAC) of the National Astronomical Observatory, Japan. YPJ is supported in part by NKBRSF (G19990754) and by NSFC.

## REFERENCES

- Benson A.J., Lacey C.G., Baugh C.M., Cole S., Frenk C.S., 2002, MNRAS, 333, 156
- Berlind A.A., Weinberg D.H., 2002, ApJ, 575, 587
- Bromley B.C., Press W.H., Lin H., Kirshner R.P., 1998, ApJ, 505, 25B
- Bullock J.S., Wechsler R.H., Somerville R.S., 2002, MNRAS, 329, 246
- Colless M., et al., 2001, MNRAS, 328, 1039
- De Propris R., Colless M., Driver S.P., Couch W., Peacock J.A., et al., 2003, MNRAS, 342, 725
- Gottloeber S., Lokas E., Klypin A., Hoffman Y., 2003, astro-ph/0305393, submitted to MNRAS
- Hoyle F., Rojas R.R., Vogeley M.S., Brinkmann J., 2003, astro-ph/0309728, submitted to ApJ
- Hütsi G., Einasto J., Tucker D.L., Saar E., Einasto M., Müller V., Heinämäki P., Allam S.S., 2002, astro-ph/0212327, submitted to A&A
- Jing Y.P., Mo H.J., Börner G., 1998, ApJ, 494, 1
- Jing Y.P., Suto, Y., 2002, ApJ, 574, 538
- Kang X., Jing Y.P., Mo H.J., Börner G., 2002, MNRAS, 336, 892
- Kauffmann G., Colberg J.M., Diaferio A., White S.D.M., 1999, MNRAS, 303, 188
- Kravtsov A.V., Berlind A.A., Wechsler R.H., Klypin A.A., Gottloeber A., Allgood B., Primack J.R., 2003, astro-ph/0308519, submitted to ApJ
- Lemson G., Kauffmann G., 1999, MNRAS, 302, 111
- Magliocchetti M., Porciani C., 2003, preprint (astro-ph/0304003)

<sup>†</sup> During the final stages of this project, Hoyle et al (2003) published a paper based on SDSS data that addresses the environment-dependence of the LF. Their results are qualitatively in good agreement with our predictions, though we delay a more detailed comparison to a future paper.



- Mathis H., White S.D.M., 2002, MNRAS, 2002, MNRAS, 337, 1193
- Mathis H., Lemson G., Springel V., Kauffmann G., White S.D.M., Eldar A., Dekel A., 2002, MNRAS, 333, 739
- Mo H.J., White S.D.M., 1996, MNRAS, 282, 347
- Peacock J.A., Smith R.E., 2000, MNRAS, 318, 1144
- Scoccimarro R., Sheth R.K., Hui L., Jain B., 2001, ApJ, 546, 20
- Seljak U., 2000, MNRAS, 318, 203
- Scranton R., 2002, MNRAS, 332, 697
- Sheth R.K., Tormen G., 1999, MNRAS, 308, 119
- Sheth R.K., Mo H.J., Tormen G., 2001, MNRAS, 323, 1
- Sheth R.K., Tormen G., 2002, MNRAS, 329, 61
- Somerville R.S., Primack J.R., 1999, MNRAS, 310, 1087
- Spergel D.N., et al., 2003, preprint (astro-ph/0302209)
- van den Bosch F.C., Yang X.H., Mo H.J., 2003a, MNRAS, 340, 771 (Paper II)
- van den Bosch F.C., Mo H.J., Yang X.H., 2003b, MNRAS, in press (astro-ph/0301104)
- van den Bosch F.C., Norberg P., Mo H.J., Yang X.H., Jing Y.P., 2004, in preparation
- White S.D.M., Rees M.J., 1978, MNRAS, 183, 341
- Yan R., Madgwick D.S., White M., 2003, preprint (astro-ph/0307248)
- Yang X.H., Mo H.J., van den Bosch F.C., 2003a, MNRAS, 339, 1057 (Paper I)
- Yang X.H., Mo H.J., Jing Y.P., van den Bosch F.C., Chu Y.Q., 2003b, MNRAS, in press (astro-ph/0303524)
- York D., et al., 2000, AJ, 120, 1579
- Zehavi I., et al., 2003, preprint (astro-ph/0301280)
- Zheng Z., Tinker J.L., Weinberg D.H., Berlind A.A., 2002, ApJ, 575, 617